SEMARAK ILMU PUBLISHING

Journal of Advanced Research in Fluid Mechanics and Thermal Sciences

Journal homepage:
https://semarakilmu.com.my/journals/index.php/fluid_mechanics_thermal_sciences/index
ISSN: 2289-7879

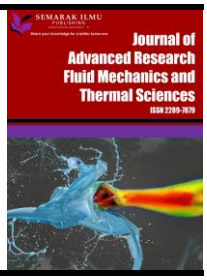

Non-Newtonian Fluid Film Lubrication of Asymmetric Rollers using Vogel Viscosity-Temperature Relationship

Swetha Lanka[1,2], Venkata Subrahmanyam Sajja[1,*], Dhaneshwar Prasad[3]

[1] Department of Engineering Mathematics, Koneru Lakshmaiah Education Foundation, Guntur-522302, A.P., India
[2] Department of Mathematics, Sir C R Reddy College of Engineering, Eluru-534007, A.P., India
[3] Department of Mathematics, Kanchi Mamunivar Government Institute for Post Graduate Studies and Research, Puducherry-605008, India

ARTICLE INFO

Article history:
Received 3 July 2023
Received in revised form 20 September 2023
Accepted 29 September 2023
Available online 18 October 2023

Keywords:
Hydrodynamic lubrication; thermal effects; non-Newtonian; Bingham plastic; in-compressible; viscosity

ABSTRACT

A theoretical analysis of asymmetric roller bearing system with cavitation that is hydro-dynamically lightly loaded and lubricated by a thin, in-compressible fluid is presented. The lubricant adheres to the non-Newtonian Bingham plastic fluid concept, in which the viscosity of the fluid should change depending on the mean film temperature. The continuity and momentum equations, which regulate fluid flow, are first solved analytically and then numerically using MATLAB. Through graphs and tables, some key bearing features are addressed and further explained. This leads to the conclusion that there is a discernible difference between Newtonian and non-Newtonian fluids in terms of pressure, temperature, load, and traction. The findings are good in line with the body of literature.

1. Introduction

Many technical fields depend on the fluid film lubrication technique, which is widely used in machine devices, motors, super gadgets, cams and skeletal joints. Regardless, exploratory outcomes show that the expansion of modest quantities of since quite a while ago fastened added substances to a Newtonian lubricant restricts the affectability of the oil to change in shear rate and gives advantageous repercussions for the store passing on and frictional qualities [1].

On surfaces that are subject to fluid scouring, hydrodynamic lubrication is a technique used to reduce wear and friction. Adding the right liquid with the intention that it penetrates the contact area between the scouring surfaces and creates a thin layer is the typical purpose of hydrodynamic lubrication. This coating effectively lowers friction and wear by keeping the surfaces from coming into touch. Extremely high loads, peak speeds, and extreme slip situations are ongoing demands placed on bearings. For example, the viscosity of oil varies continuously with temperature and pressure in the high-pressure area [2].

* *Corresponding author.*
E-mail address: subrahmanyam@kluniversity.in

https://doi.org/10.37934/arfmts.110.2.3248

The steady state lubrication of two rigid cylindrical rollers under entraining and squeezing motion including cavitation is studied by Sinha and Prasad [3]. The lubricant consistency m of the power law fluid is assumed to be pressure and temperature dependent. A numerical solution to the coupled Reynolds' and energy equation for pressure and temperature has been obtained using higher order predictor corrector method. The variation in consistency is found to be very significant, especially in the pressure peak region. Prasad *et al.,* [2] published a study on the thermo-hydrodynamic lubrication of line contact using an incompressible power-law fluid. There is a significant difference between Newtonian and non-Newtonian fluids in terms of temperature, pressure, load, and traction, according to the pressure and heat equations, which depend on consistency, rolling ratio, and power-law parameter. In order to investigate the thermo-hydrodynamic effect for substantially loaded journal bearings, Prasad *et al.,* [1] used the power-law model. The load ratio drops with rise in the power-law index "n," which is based on the assumption that the lubricant's consistency changes with both pressure and also mean temperature. Using in-compressible, power-law lubricants, including Newtonian, in isothermal and adiabatic conditions, Sajja and Prasad [4] investigated the theoretical characterization of HDL of anti-symmetric surfaces. The load with the flow index 'n' and pressure both significantly increase for a constant value of the rolling ratio parameter, it is inferred.

In addition, in most of the classical problems lubricant is assumed to be Newtonian. However, since the lubricant is subject to extremely high pressure and shear stresses, as in the case of gear – meshes, heavily loaded rolling element bearings, which only act for a very short time, the Newtonian behaviour of the lubricant ceases to exist [5]. Besides, many lubricants contain high molecular weight polymers that also make them strongly non-Newtonian [6]. Hence, the effect of non-Newtonian lubricant is to be incorporated along with the effects of pressure and temperature on the lubricants. The properties of non-Newtonian Bingham plastic fluid flow have long been used to describe the behaviour of fluids in general. Additionally, they have been used to show how melts and slurries behave in moulds and during designed handling [7]. Examining grease speculatively using the Bingham model and returning to Milne [8]. The basic slider bearing and journal bearing in one dimension were the subject of his investigation, and he came to the conclusion that any surface might have had rigid "cores" added to it. In addition, Christopher Dorier and John Tichy introduced a model of the behaviour of fluids that are similar to Bingham's, which exhibit a yield stress [6]. Revathi *et al.,* [9] recently investigated non-Newtonian lubrication of asymmetric rollers for a highly stacked rigid system using an incompressible Bingham plastic fluid in rolling/sliding line contact while modifying the fluid viscosity with hydrodynamic pressure. The findings, particularly the pressure, load, and traction forces, are well in line with the body of currently available literature. Distributions of lubricant velocity are produced. Additionally, Gadamsetty *et al.,* [10] investigated a topic pertaining to the lubricating properties of anti-symmetric rollers using a non-Newtonian in-compressible Bingham plastic fluid. For both Newtonian and non-Newtonian fluids, the temperatures, pressures, loads, and traction forces, in particular, are in good agreement with prior findings. Ahmed and Biancofiore [11] proposed a new approach for the numerical simulation of a three-dimensional contact lubricated by a shear thinning liquid film. This approach is based on a modification of the viscous shear thinning function. Veltkamp *et al.,* [12] developed and compared a hydrodynamic model that includes shear thinning to experimental data. The model describes the dependence on lubrication parameters well, but underestimates the lubricating layer thickness by a constant factor.

The earlier research work was carried out by the researchers taking symmetric roller bearings into consideration lubricated by non-Newtonian fluids such as power-law, micro polar, and Bingham plastic fluid, etc., under the behavior of line contact and point contact. But, much work has not been carried out by the researchers from this field taking into account the asymmetric roller bearings with viscosity as a function of temperature. Hence in the present work, the attention has been focussed

on to analyse the thermal effects of an incompressible Bingham plastic fluid used to lubricate asymmetric rollers in a lightly loaded rolling/sliding inelastic system under the behaviour of line contact. The lubricant viscosity is here considered to be a function of mean film temperature. Rolling ratios are used to assess how pressure, load, and traction are affected as surfaces slide and roll. It is presumable that the viscosity changes with mean temperature.

2. Theoretical Model

Lightly loaded rigid system with asymmetric roller bearings using non-Newtonian incompressible lubricant is considered in this work to account for the Bingham plastic fluid. Both surfaces in this study have the same radius and are moving at different velocities. The fact that the lower surface is moving faster than the upper surface is also obvious. The physical diagram of the flow pattern is presented in Figure 1.

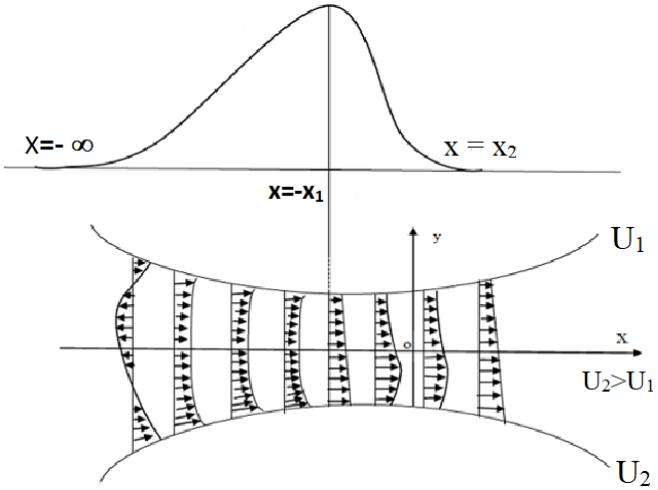

Fig. 1. Lubrication of Asymmetric Rollers

2.1 Governing Equations

Under common presumptions given by Prasad *et al.,* [13], the following governing equations, which regulate the in-compressible fluids flow, are taken into account:

$$\frac{\partial u}{\partial x}+\frac{\partial v}{\partial y}=0 \tag{1}$$

$$\frac{dp}{dx}=\frac{\partial \tau}{\partial y} \tag{2}$$

where, respectively, ‘p’ denotes hydrodynamic pressure and ‘τ’ lubricant shear stress. For Bingham plastic fluid, the fundamental equation is provided by Sasaki *et al.,* [14] as follows:

$$\tau=\pm \tau_0+\mu\frac{\partial u}{\partial y} \tag{3}$$

where μ is the lubricant viscosity-temperature relationship is given by Vogel equation [15]

$$\mu = \mu_0 e^{-\beta (T_m - T_0)} \tag{4}$$

and the equation to be used to determine the film's thickness is $h = h_0 + \frac{x^2}{2R}$ (5)

R represents the radius of the 'equivalent cylinder'.

2.2 Boundary Conditions

For this problem, the upper and lower surfaces' boundary conditions are assumed to be

$$u = U_1 \ \ at \ y = h \tag{6}$$

$$u = U_2 \ \ at \ y = -h \tag{7}$$

$$p = 0 \ \ at \ \ x = -\infty \tag{8}$$

$$p = 0 \ \ and \ \ \frac{dp}{dx} = 0 \ at \ x = x_2 \tag{9}$$

where U_1 and U_2 are speeds of the rollers.

Eq. (2) is integrated by making use of the aforementioned 'boundary conditions' to produce the fluid velocity expression shown below.

$$u = \frac{3(y^2 - h^2)(U_1 + U_2)(h - h_1)}{4h^3} - \frac{y}{2h}(U_2 - U_1) + \frac{1}{2}(U_1 + U_2) \tag{10}$$

The above velocity is integrated in the area between the surfaces to get the 'volume flux, Q' for the 'fluid flow', which is provided below

$$Q = \int_{-h}^{h} u dy = h(U_1 + U_2) - \frac{2h^3}{3\mu} \frac{dp}{dx} \tag{11}$$

And the 'volume flux' at the pressure's peak is

$$Q(-x_1) = (U_1 + U_2) h_1 \tag{12}$$

Where the 'film thickness' h_1 at $x = -x_1$ is considered to be $h_1 = 1 + x_1^2$.

2.3 Reynolds Equation

Above boundary conditions can be used to solve Eq. (2) and supply the pressure Reynolds equation as presented below.

$$\frac{dp}{dx}=\frac{3\mu}{2h^3}\left[\left(U_1+U_2\right)\left(h-h_1\right)\right] \tag{13}$$

2.4 Scheme for Non-Dimensionless

The following non-dimensional technique is utilised in this article.

$$\bar{x}=\frac{x}{R},\ \bar{p}=\frac{p}{p_r},\ \bar{\mathrm{h}}=\frac{h}{h_{\mathrm{o}}},\ \bar{y}=\frac{y}{h_{\mathrm{o}}},\bar{T}=\beta T,\ \overline{T_m}=\beta T_m,$$
$$\overline{\tau_{\mathrm{o}}}=\frac{R\tau_{\mathrm{o}}}{p_r h_{\mathrm{o}}},\ \overline{\mu_{\mathrm{o}}}=\frac{RU_1}{p_r h_{\mathrm{o}}^2}\mu_{\mathrm{o}}\ ,\ \overline{W_x}=\frac{2W_x}{Rp_r},\ \overline{W_y}=\frac{2W_y}{Rp_r},$$
$$\overline{T_{Fh+}}=\frac{T_{Fh+}}{p_r h_{\mathrm{o}}},\ \overline{T_{Fh-}}=\frac{T_{-Fh}}{p_r h_{\mathrm{o}}},\ \overline{\mu}=\overline{\mu_{\mathrm{o}}}e^{-\left(\overline{T_m}-\overline{T_{\mathrm{o}}}\right)}$$

Using the aforementioned dimensionless technique, the velocity and pressure equation are represented in dimensionless form.

$$\bar{u}=\frac{3\left(1+\bar{U}\right)\left(\bar{h}-\overline{h_1}\right)\left(\bar{y}^2-\bar{h}^2\right)}{4\bar{h}^3}+\frac{\bar{y}}{2\bar{h}}\left(1-\bar{U}\right)+\frac{1}{2}\left(1+\bar{U}\right) \tag{14}$$

$$\frac{d\bar{p}}{d\bar{x}}=\frac{3\bar{\mu}\left(1+\bar{U}\right)\left(\bar{h}-\overline{h_1}\right)}{4\bar{h}^3} \tag{15}$$

2.5 Heat Equation

Assume the line contact lubrication problem with the following heat equation [3]:

$$\rho c_p\left(u_m\frac{dT_m}{dx}\right)=k\frac{\partial^2 T}{\partial y^2}+\tau\frac{\partial u}{\partial y} \tag{16}$$

Eq. (3) is used to derive the shear stress for the Bingham plastic fluid.

The following describe the heat equation's boundary conditions.

$$\frac{\partial T}{\partial y}=0\ at\ y=h\ and\ T=T_L\ at\ y=-h \tag{17}$$

The temperature of the lubricant is shown below as a result of integration of Eq. (16):

$$T = T_L + \left(\frac{\rho c_p}{2k}\right)\left(u_m \frac{dT_m}{dx}\right)\left(y^2 - 2hy - 3h^2\right) - \left(\frac{\tau_0}{k}\right)\left[\left(\frac{U_1 - U_2}{4h}\right)\left(y^2 - 2hy - 3h^2\right) + \left(\frac{(U_1 + U_2)(h - h_1)}{4h^3}\right)\left(y^3 - 3h^2 y - 2h^3\right)\right]$$
$$- \left(\frac{\mu}{k}\right)\left[\left(\frac{(U_1 - U_2)^2}{8h^2}\right)\left(y^2 - 2hy - 3h^2\right) + \left(\frac{3(U_1 + U_2)^2 (h - h_1)^2}{16h^6}\right)\left(y^4 - 4h^3 y - 5h^4\right) + \left(\frac{(U_1 - U_2)(U_1 + U_2)(h - h_1)}{4h^4}\right)\left(y^3 - 3h^2 y - 2h^3\right)\right] \quad (18)$$

Thus, the explicit relationship between x and y and the temperature 'T' is known analytically. The mean film temperature is now provided by $T_m = \frac{1}{2h}\int_{-h}^{h} T dy$ and obtained as:

$$T_m = T_L - \left(\frac{4\rho c_p h^2}{3k}\right)\left(u_m \frac{dT_m}{dx}\right) + \left(\frac{\tau_0}{k}\right)\left[\left(\frac{2(U_1 - U_2)h}{3}\right) + \left(\frac{(U_1 + U_2)(h - h_1)}{2}\right)\right]$$
$$+ \left(\frac{\mu}{k}\right)\left[\left(\frac{(U_1 - U_2)^2}{3}\right) + \left(\frac{9(U_1 + U_2)^2 (h - h_1)^2}{10h^2}\right) + \left(\frac{(U_1 - U_2)(U_1 + U_2)(h - h_1)}{2h}\right)\right] \quad (19)$$

Now, the 'temperature and mean temperature' in dimensionless form are produced as shown below:

$$\bar{T} = \bar{T}_L + \left(\bar{P}_e \frac{d\bar{T}_m}{d\bar{x}}\right)\left(\bar{y}^2 - 2\bar{h}\bar{y} - 3\bar{h}^2\right) - \left(\bar{P}_R \bar{E}_t\right)\left[\bar{\eta} A_1(x) + \bar{\mu} A_2(x)\right] \quad (20)$$

$$\bar{T}_m = \bar{T}_L - \left(\frac{8\bar{h}^2}{3}\bar{P}_e \frac{d\bar{T}_m}{d\bar{x}}\right) + \bar{P}_R \bar{E}_t \left[\bar{\eta} A_3(x) + \bar{\mu} A_4(x)\right] \quad (21)$$

$$\frac{d\bar{T}_m}{d\bar{x}} = \frac{3}{8\bar{h}^2 \bar{P}_e}\left[\bar{T}_L - \bar{T}_m + \bar{P}_R \bar{E}_t \left[\bar{\eta} A_3(x) + \bar{\mu} A_4(x)\right]\right] \quad (22)$$

Where

$$A_1(x) = \left[\left(\frac{\left(1 - \bar{U}\right)}{4\bar{h}}\right)\left(\bar{y}^2 - 2\bar{h}\bar{y} - 3\bar{h}^2\right) + \left(\frac{\left(1 + \bar{U}\right)\left(\bar{h} - \bar{h}_1\right)}{4\bar{h}^3}\right)\left(\bar{y}^3 - 3\bar{h}^2\bar{y} - 2\bar{h}^3\right)\right]$$

$$A_2(x) = \left[B_1(x) + B_2(x) + B_3(x)\right]$$

$$B_1(x) = \left(\left(\frac{\left(1 - \bar{U}\right)^2}{8\bar{h}^2}\right)\left(\bar{y}^2 - 2\bar{h}\bar{y} - 3\bar{h}^2\right)\right.$$

$$B_2(x)=\left(\left(\frac{3\left(1+\bar{U}\right)^2\left(\bar{h}-\bar{h_1}\right)^2}{16\,\bar{h}^6}\right)\left(\bar{y}^4-4\bar{h}^3\bar{y}-5\bar{h}^4\right)\right)$$

$$B_3(x)=\left(\left(\frac{\left(1-\bar{U}\right)\left(1+\bar{U}\right)\left(\bar{h}-\bar{h_1}\right)}{4\,\bar{h}^4}\right)\left(\bar{y}^3-3\bar{h}^2\bar{y}-2\bar{h}^3\right)\right)$$

$$A_3(x)=\left[\left(\frac{2\left(1-\bar{U}\right)\bar{h}}{3}\right)+\left(\frac{\left(1+\bar{U}\right)\left(\bar{h}-\bar{h_1}\right)}{2}\right)\right]$$

$$A_4(x)=\left[\left(\frac{\left(1-\bar{U}\right)^2}{3}\right)+\left(\frac{9\left(1+\bar{U}\right)^2\left(\bar{h}-\bar{h_1}\right)^2}{10\bar{h}^2}\right)+\left(\frac{\left(1+\bar{U}\right)\left(1-\bar{U}\right)\left(\bar{h}-\bar{h_1}\right)}{2\bar{h}}\right)\right]$$

$$\bar{\gamma}=\frac{\beta p_r U_1 h_0^2}{KR}=\left(\frac{c_p h_0^2 p_r}{KU_1 R}\right)\left(\frac{\beta U_1^2}{c_p}\right)=\overline{P_R}\;\overline{E_t}$$

$$\bar{P}_e=\left(\frac{\rho c_p u_m h_0^2}{2KR}\right)\quad;\quad\bar{\eta}=\left(\frac{R\tau_0}{h_0 p_r}\right)$$

2.6 Load and Traction [3]

Since load capacity produces complete estimation of the bearing's efficiency, so load capacity is the one of the significant qualities. Hence, Integration of the pressure across the film thickness gives the x-component of the load W_x per unit length of the cylinder as

$$W_x=-\int_{-h}^{h}p\,dh \tag{23}$$

The dimensionless normal load $\overline{W_x}$ is given by

$$\overline{W}_x=\int_{-\infty}^{\bar{x}_2}\bar{x}^{-2}\,\frac{d\bar{p}}{d\bar{x}}\,d\bar{x} \tag{24}$$

Similarly, the normal load carrying capacity Wy can be obtained as

$$W_y=\int_{-\infty}^{x_2}p\,dx \tag{25}$$

The dimensionless normal load $\overline{W_y}$ is given by

$$\overline{W}_y = -\int_{-\infty}^{\bar{x}_2} 2\bar{x}\,\frac{d\bar{p}}{d\bar{x}}\,d\bar{x} \tag{26}$$

The load component in dimensionless form is given by

$$\overline{W} = \sqrt{\overline{W}_x^2 + \overline{W}_y^2} \tag{27}$$

Further, Integration of the shear stress 'τ' for the entire length gives the traction force 'T_F' at the surfaces can be obtained as

$$T_{Fh-} = -\int_{-\infty}^{x_2} \tau_{y=-h}\,dx \text{ and } T_{Fh+} = -\int_{-\infty}^{x_2} \tau_{y=h}\,dx \tag{28}$$

The tractions in non-dimensional form are

$$\bar{T}_{Fh} = -\int_{-\infty}^{\bar{x}_2}\left[\bar{\tau}_0 + \left(\frac{\bar{\mu}}{2\bar{h}}\right)\left[\left(1-\bar{U}\right) + \left(\frac{3\left(1+\bar{U}\right)\left(\bar{h}-\bar{h}_1\right)}{\bar{h}}\right)\right]\right]d\bar{x} \tag{29}$$

$$\bar{T}_{Fh-} = -\int_{-\infty}^{\bar{x}_2}\left[\bar{\tau}_0 + \left(\frac{\bar{\mu}}{2\bar{h}}\right)\left[\left(1-\bar{U}\right) - \left(\frac{3\left(1+\bar{U}\right)\left(\bar{h}-\bar{h}_1\right)}{\bar{h}}\right)\right]\right]d\bar{x} \tag{30}$$

3. Results and Discussion

In this problem, numerical calculations are made using the following values:

$$U_1 = 400\ cm/s,\ h_0 = 4\times10^{-4}\ cm,\ R = 3\ cm,\ \overline{T_L} = 1.5$$

3.1 Velocity Profile

Figure 2 and 3 display the fluid's velocity for the regions prior to, following, and at the point where the pressure peaks, respectively. The profiles in the first two graphs resemble parabolas with vertices pointing upward and downward in the areas prior to and after the point of pressure peak. As seen in Figure 2, the vertices under the $\bar{y}$ line indicate that there is a reverse flow at the inlet. The back flow is over as the fluid progresses in the gap between the rollers. Prasad and Sajja [16] demonstrated reverse flow. The back flow is eliminated as the fluid moves forward [10,16-18]. However, the velocity profile, which can be seen in Figure 4, appears to be increasing linearly at the point of maximum pressure [13]. This is because of that upper surface is moving with high velocity.

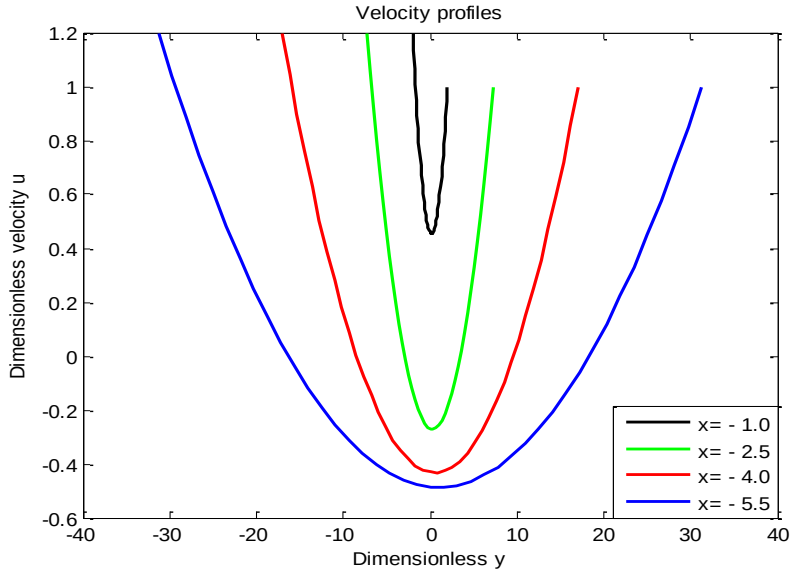

Fig. 2. Velocity profile

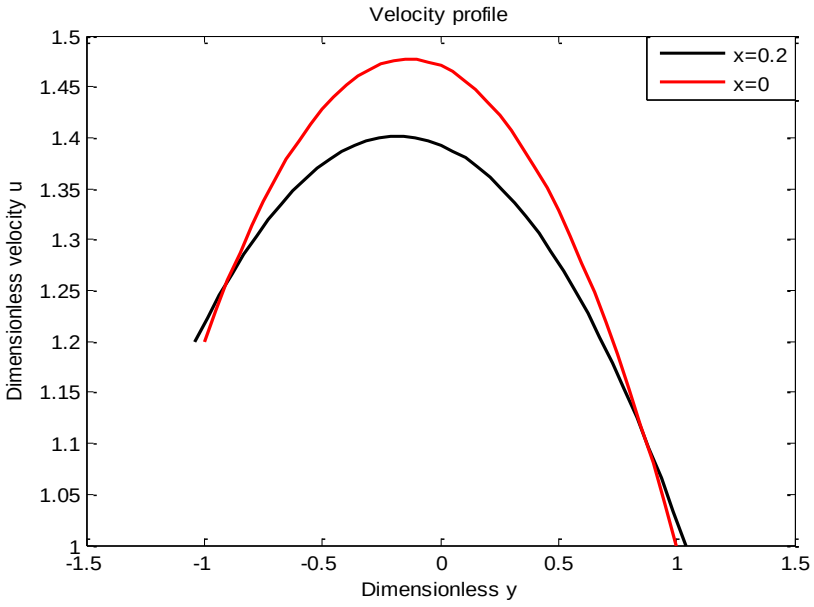

Fig. 3. Velocity profile

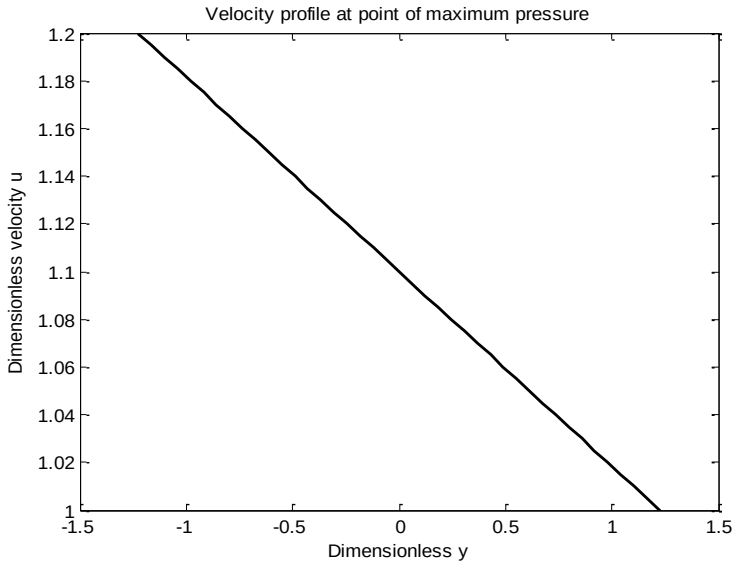

Fig. 4. Velocity at pressure peak point

3.2 Pressure Profile

The dimensionless pressure $\overline{p}$ are quantitatively estimated and shown in Figure 5 to Figure 7. Figure 5 and 6 show that in the Newtonian ($\overline{\tau_0}=0$) and non-Newtonian ($\overline{\tau_0}\neq 0$) instances, respectively, $\overline{p}$ rises as rolling ratio $\overline{U}$ rises. It shows that, in comparison to pure rolling, hydrodynamic pressure is greater in the sliding scenario. These behaviours have been seen in the previous studies [5,6,16,19,20]. In addition, the lubricant pressure for distinct values of τ_0 is depicted in Figure 7 for the sliding case. It is clear from this figure that Newtonian fluids experience greater pressure than non-Newtonian fluids. The cavitation points for both Newtonian and non-Newtonian fluids are also shown in Table 1. This table shows that as the rolling ratio rises, the cavitation points move away from the centre line of contact, for $\overline{\tau_0}=1$ and $\overline{\tau_0}=0$ respectively. Revathi *et al.,* [9] demonstrates similar kind of behaviour.

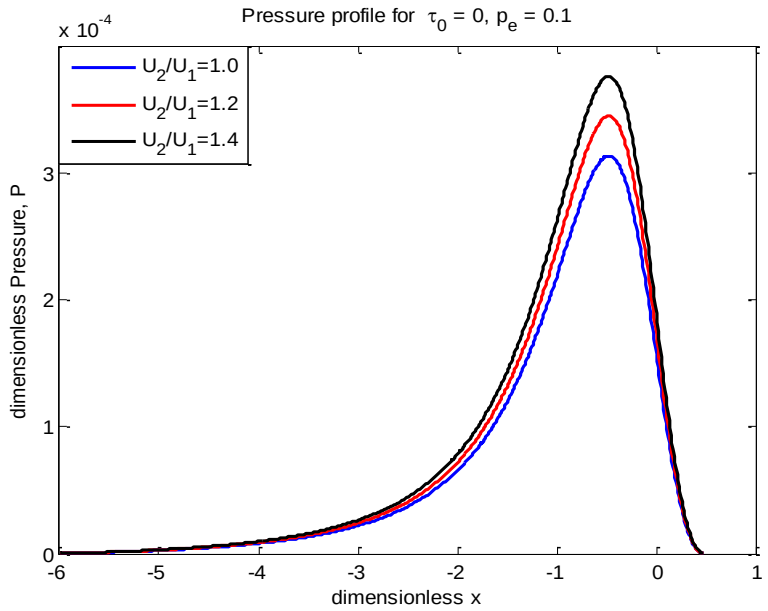

Fig. 5. Pressure profile

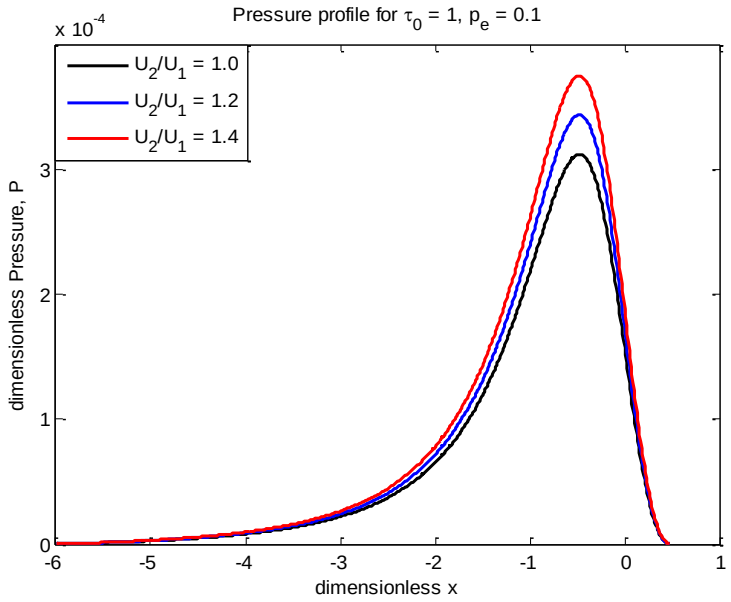

Fig. 6. Pressure profile

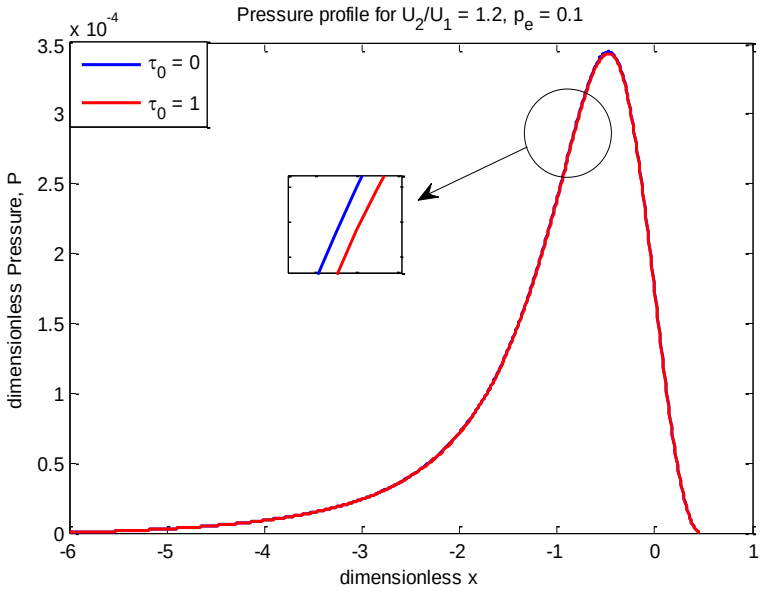

Fig. 7. Pressure profile

Table 1
Cavitation Points

$\overline{U}$	$\overline{\tau_0}=0$	$\overline{\tau_0}=1$
1.0	0.4750595623	0.4748092764
1.1	0.4751002839	0.4748323062
1.2	0.4751931247	0.4749094165
1.3	0.4753476251	0.4750705201
1.4	0.4755643208	0.4752714923
1.5	0.4758302315	0.4755143814

3.3 Viscosity ($\overline{\mu}$) Profile

Figure 8 to Figure 10 show the numerically calculated dimensionless viscosity for different values of rolling ratio $\overline{U}$, yield stress parameter $\overline{\tau_0}$, and peclet number $\overline{p_e}$. The dimensionless viscosity for non-Newtonian case is calculated numerically for different values of $\overline{U}$ and presented in the Figure 8. It can be observed from the figure that the viscosity increases for increasing values of sliding parameter $\overline{U}$. This is because of pressure and pressure increase, viscosity increases. This is in conformity with the results of Gadamsetty *et al.,* [21]. For distinct values of $\overline{\tau_0}$ in the sliding case, the viscosity $\overline{\mu}$ is estimated numerically and presented in Figure 9. The figure shows that the viscosity for the Newtonian case is greater than that of the non-Newtonian case. The viscosity in the beginning at the inlet region is high for non-Newtonian fluid, but later the trend was reversed. The viscosity for different values of $\overline{p_e}$ is depicted in Figure 10 and observed that viscosity is increasing for increasing values of $\overline{p_e}$.

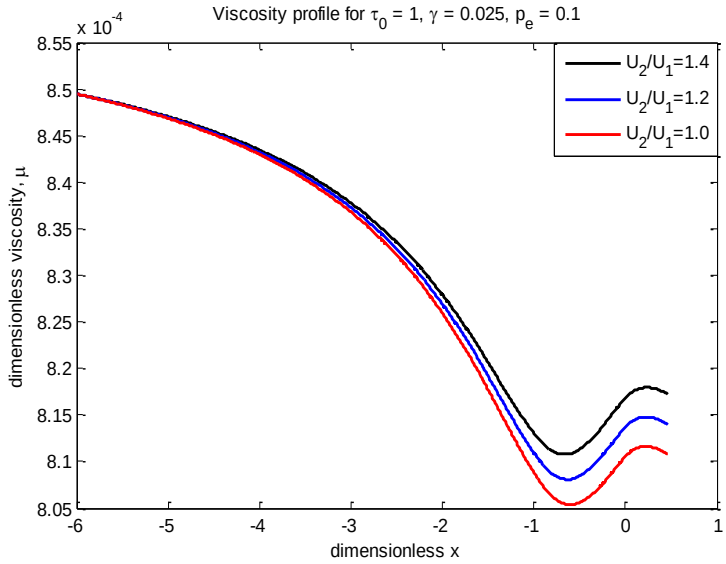

Fig. 8. Viscosity profile

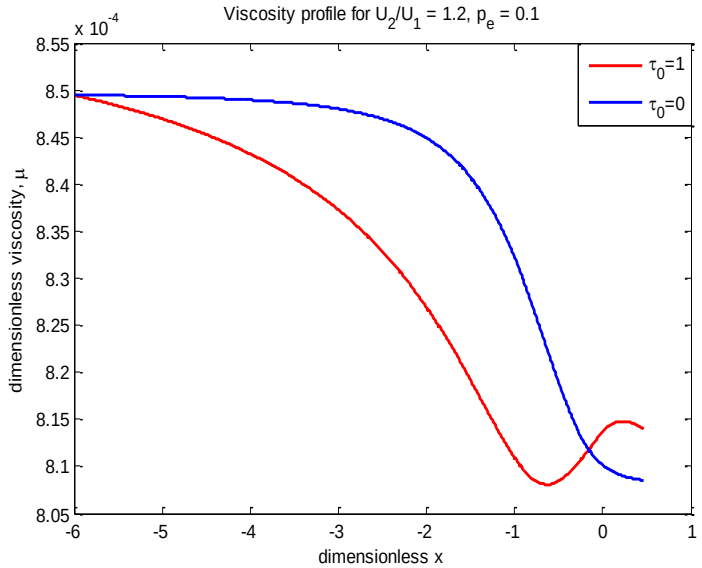

Fig. 9. Viscosity profile

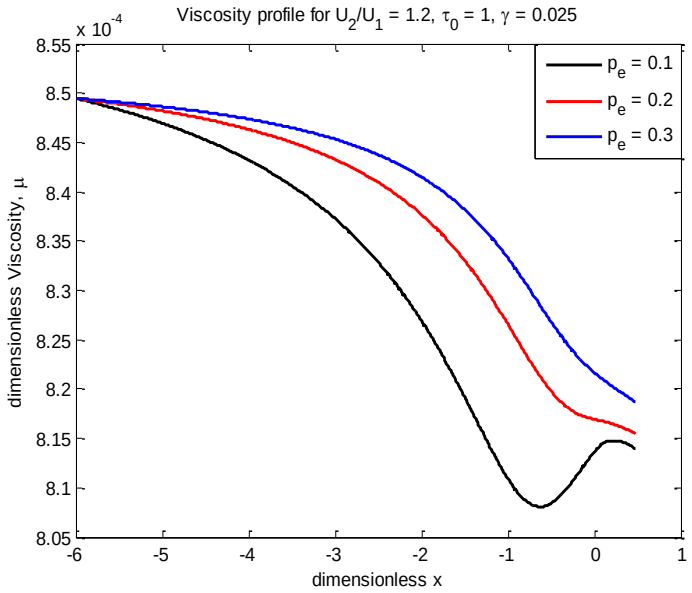

Fig. 10. Viscosity profile

3.4 Mean Temperature Profile

Figure 11 to 14 show the dimensionless mean temperature $\overline{T_m}$ of the lubricant for various values of rolling ratio parameter $\overline{U}$ and yield stress parameter $\overline{\tau_0}$. Figure 11, which shows the dimensionless mean temperature for distinct values of $\overline{U}$ for $\overline{\tau_0}=0$ (Newtonian case), demonstrates that the mean temperature increases for increasing values of $\overline{U}$. This indicates that the sliding temperature is higher than that of pure rolling. This result is matching with the previous findings of [4,10,18]. When non-Newtonian fluid is considered the mean temperature, depicted in Figure 12, drops as $\overline{U}$ increases. This is because of the viscosity relation considered in this work. Figure 13 represents the mean temperature profile for sliding case for different values of yield stress parameter $\overline{\tau_0}$ and it can be seen from this figure that mean temperature is higher in the in-let region for non-Newtonian fluid, later it was reversed. The mean temperature for different values of peclet number $\overline{p_e}$ is calculated for sliding case and presented in Figure 14. It demonstrates from this figure that mean temperature decreases as $\overline{p_e}$ increases. This kind of behavior can be observed in a study by Prasad and Sajja [16]. It may be noted that the mean temperature refers to the case without convection when $\overline{p_e}\to 0$.

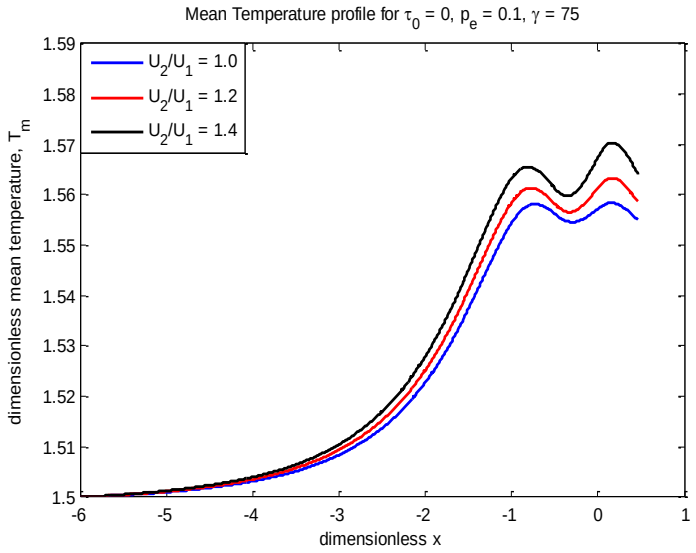

Fig. 11. Mean Temperature profile

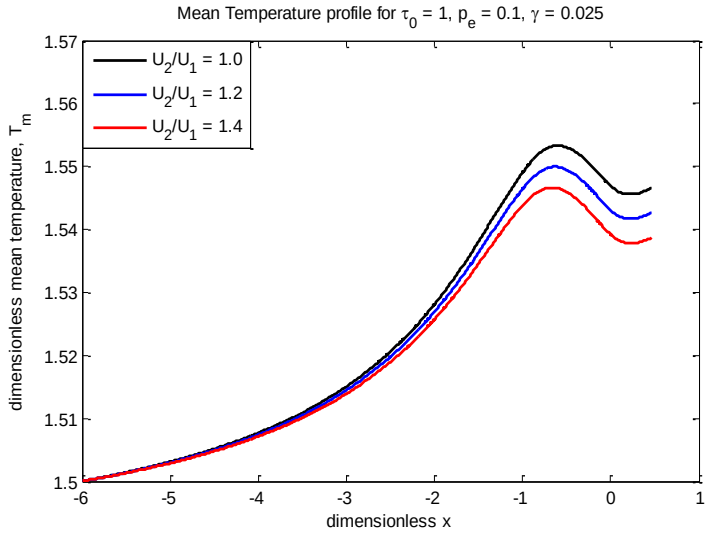

Fig. 12. Mean Temperature profile

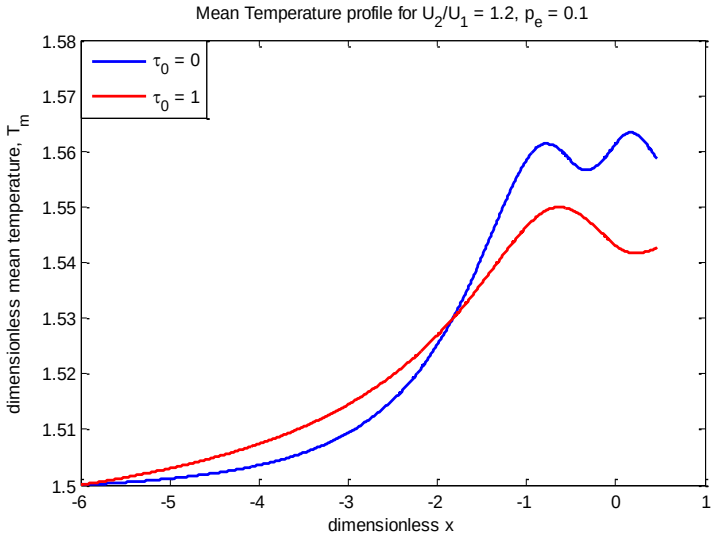

Fig. 13. Mean Temperature profile

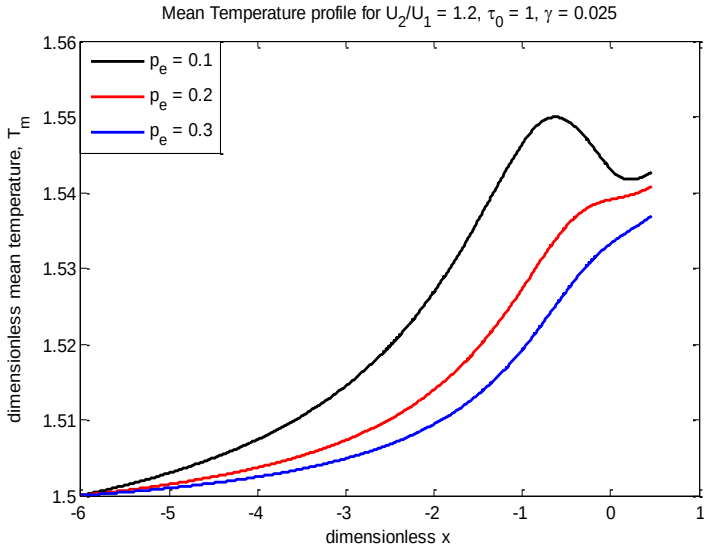

Fig. 14. Mean Temperature profile

3.5 Load and Traction

For various values of the rolling ratio $\overline{U}$ and yield stress parameter $\overline{\tau}_0$, dimensionless load values in the y-direction are calculated and shown in Table 2. The table also demonstrates that, in both Newtonian and non-Newtonian scenarios, load rises with rolling ratio. This is because of lubricant pressure and load is function of pressure. These findings are fairly consistent with past research findings [16-18,20]. Further, the Newtonian load is more when compared with Newtonian load for any fixed values of rolling ratio parameter $\overline{U}$.

Table 2
Load $\overline{W}$ values

$\overline{U}$	$\overline{\tau_0}=0$	$\overline{\tau_0}=1$
1.0	0.00067970	0.00067735
1.1	0.00071366	0.00071132
1.2	0.00074762	0.00074533
1.3	0.00078159	0.00077932
1.4	0.00081556	0.00081331
1.5	0.00084953	0.00084732

Table 3 and 4 show the computed traction forces at the lower and upper surfaces for various values of $\overline{\tau}_0$ and $\overline{U}$. Both the Newtonian and non-Newtonian cases are shown for $\overline{\tau}_0=0$ and $\overline{\tau}_0=1$ respectively here. For a certain value of $\overline{U}$, the traction forces grow on the lower and higher surfaces with $\overline{\tau}_0$. Table 3 also shows that traction forces rise with $\overline{U}$, which suggests that traction forces will be higher on surfaces moving faster. These results closely resemble those found in the studies by Gadamsetty *et al.,* [10,21]. When running at the same speed, both rollers attain the same traction force. Further, Table 4 show the traction values drops as $\overline{U}$ increases. This is due to the lower speed of the upper surface.

Table 3
Traction values at lower surface

$\overline{U}$	$\bar{\tau}_0=0$	$\bar{\tau}_0=0.5$	$\bar{\tau}_0=1$
1.0	0.00429290	2.29429706	4.58430084
1.1	0.00485796	2.29486273	4.58486694
1.2	0.00542298	2.29542830	4.58543330
1.3	0.00598812	2.29599390	4.58599938
1.4	0.00655324	2.29655953	4.58656548
1.5	0.00711838	2.29712516	4.58713162

Table 4
Traction values at upper surface

$\overline{U}$	$\bar{\tau}_0=0$	$\bar{\tau}_0=0.5$	$\bar{\tau}_0=1$
1.0	0.00429290	2.29429706	4.58430084
1.1	0.00415659	2.29416137	4.58416558
1.2	0.00402025	2.29402557	4.58403057
1.3	0.00388403	2.29388980	4.58389529
1.4	0.00374778	2.29375407	4.58376001
1.5	0.00361155	2.29361833	4.58362480

4. Conclusion

An attempt is made to investigate the non-Newtonian in-compressible Bingham plastic fluid film lubrication properties of the line contact problem for lightly loaded rigid system. For various values of the yield stress and sliding parameters, the governing equations are solved for pressure, mean film temperature and velocity of the lubricant. The outcomes of this work can be used to support the following assertions.

i. The velocity of the lubricant is independent of $\bar{\tau}_0$.
ii. Lubricant velocity at point of pressure peak decreases linearly.
iii. Pressure increases because of an increase in rolling ratio.
iv. The load increases as the rolling ratio rises.
v. The lower surface has greater traction than the upper surface due to its more speed.
vi. Traction forces on both surfaces increase as the yield stress parameter increases.

Acknowledgement

The investigators remain profusely grateful to Koneru Lakshmaiah Education Foundation, Guntur for extending support and assistance with required permissions during this research study at the Department of Mathematics and to Sir C R Reddy College of Engineering, Eluru for necessary permissions and extending facilities for the work. This research was not funded by any grant.

References

[1] Prasad, Dhaneshwar, Sudam Sekhar Panda, and S. V. Subrahmanyam. "Non-Newtonian squeeze film lubrication of journal bearing with temperature effect." *International Journal of Engineering Science & Advanced Technology* 2, no. 3 (2012): 438-444.

[2] Prasad, Dhaneshwar, S. V. Subrahmanyam, and Sudam Sekhar Panda. "Thermal Effects in Hydrodynamic Lubrication of Asymmetric Rollers Using Runge Kutta Fehlberg Method." *International Journal of Engineering Science & Advanced Technology* 2, no. 3 (2012): 422-437.

[3] Sinha, P., and D. Prasad. "Lubrication of rollers by power law fluids considering consistency-variation with pressure and temperature." *Acta Mechanica* 111, no. 3-4 (1995): 223-239. https://doi.org/10.1007/BF01376932

[4] Sajja, Venkata Subrahmanyam, and Dhaneshwar Prasad. "Characterization of lubrication of asymmetric rollers including thermal effects." *Industrial Lubrication and Tribology* 67, no. 3 (2015): 246-255. https://doi.org/10.1108/ILT-04-2013-0048
[5] Hirst, W., and A. J. Moore. "Elastohydrodynamic lubrication at high pressures." *Proceedings of the Royal Society of London. A. Mathematical and Physical Sciences* 360, no. 1702 (1978): 403-425. https://doi.org/10.1098/rspa.1978.0076
[6] Bourgin, Patrick. "Fluid-Film Flows of Differential Fluids of Complexity n Dimensional Approach-Applications to Lubrication Theory." *Journal of Lubrication Technology* 101, no. 2 (1979): 140-144. https://doi.org/10.1115/1.3453294
[7] Dorier, Christopher, and John Tichy. "Behavior of a Bingham-like viscous fluid in lubrication flows." *Journal of Non-Newtonian Fluid Mechanics* 45, no. 3 (1992): 291-310. https://doi.org/10.1016/0377-0257(92)80065-6
[8] Milne, A. A. "Theory of Rheodynamic Lubrication." *Kolloid-Zeitschrift* 139 (1954): 96-101. https://doi.org/10.1007/BF01502330
[9] Revathi, Gadamsetty, Venkata Subrahmanyam Sajja, and Dhaneshwar Prasad. "Bingham plastic fluid film lubrication of asymmetric rollers." *International Journal of Scientific & Technology Research* 8, no. 11 (2019): 2549-2554.
[10] Gadamsetty, Revathi, Venkata Subrahmanyam Sajja, P. Sudam Sekhar, and Dhaneshwar Prasad. "Thermal effects in Bingham plastic fluid film lubrication of asymmetric rollers." *Frontiers in Heat and Mass Transfer (FHMT)* 15, no. 18 (2020). https://doi.org/10.5098/hmt.15.18
[11] Ahmed, H., and Luca Biancofiore. "A modified viscosity approach for shear thinning lubricants." *Physics of Fluids* 34, no. 10 (2022). https://doi.org/10.1063/5.0108379
[12] Veltkamp, B., J. Jagielka, K. P. Velikov, and Daniel Bonn. "Lubrication with non-newtonian fluids." *Physical Review Applied* 19, no. 1 (2023): 014056. https://doi.org/10.1103/PhysRevApplied.19.014056
[13] Prasad, Dhaneshwar, Punyatma Singh, and Prawal Sinha. "Thermal and squeezing effects in non-Newtonian fluid film lubrication of rollers." *Wear* 119, no. 2 (1987): 175-190. https://doi.org/10.1016/0043-1648(87)90107-4
[14] Sasaki, Tokio, Haruo Mori, and Norio Okino. "Fluid lubrication theory of roller bearing-part i: fluid lubrication theory for two rotating cylinders in contact." *Journal of Basic Engineering* 84, no. 1 (1962): 166-174. https://doi.org/10.1115/1.3657240
[15] Wang, Q. Jane, and Yip-Wah Chung. *Encyclopedia of tribology*. Springer US, 2013. https://doi.org/10.1007/978-0-387-92897-5
[16] Prasad, Dhaneshwar, and Venkata Subrahmanyam Sajja. "Non-Newtonian lubrication of asymmetric rollers with thermal and inertia effects." *Tribology Transactions* 59, no. 5 (2016): 818-830. https://doi.org/10.1080/10402004.2015.1107927
[17] Prasad, Dhaneshwar, Punyatma Singh, and Prawal Sinha. "Nonuniform temperature in non-Newtonian compressible fluid film lubrication of rollers." *Journal of Tribology* 110, no. 4 (1988): 653-658. https://doi.org/10.1115/1.3261708
[18] Prasad, Dhaneshwar, J. B. Shukla, P. Singh, P. Sinha, and R. P. Chhabra. "Thermal effects in lubrication of asymmetrical rollers." *Tribology International* 24, no. 4 (1991): 239-246. https://doi.org/10.1016/0301-679X(91)90050-J
[19] Revathi, Gadamsetty, Venkata Subrahmanyam Sajja, and Dhaneshwar Prasad. "Thermal Effects in Power-law fluid film lubrication of Rolling/Sliding Line Contact." *International Journal of Innovative Technology and Exploring Engineering* 8, no. 9 (2019): 277-283. https://doi.org/10.35940/ijitee.H7195.078919
[20] Prasad, Dhaneshwar, and Venkata Subrahmanyam Sajja. "Thermal effects in non-newtonian lubrication of asymmetric rollers under adiabatic and isothermal boundaries." *International Journal of Chemical Sciences* 14, no. 3 (2016): 1641-1656.
[21] Gadamsetty, Revathi, Venkata Subrahmanyam Sajja, P. Sudam Sekhar, and Dhaneshwar Prasad. "Squeeze Film Lubrication of Asymmetric Rollers by Bingham Plastic Fluid." *Frontiers in Heat and Mass Transfer (FHMT)* 16, no. 7 (2021). https://doi.org/10.5098/hmt.16.7